Journal of Mechanical Research and Application (JMRA), Vol. 15 No.3, 1404 (2025),1-30

JMRA
Journal of Mechanical Research and Application
ISSN: 2251-7383, eISSN: 2251-7391

Determining the effect of graphene quantum dots nanoparticles on the hardness and flexural strength of SiC

Hossein Kia[1]*, Pouya Pirali[1], Hamidreza Baharvandi[1]

1-Faculty of Materials and Manufacturing Technologies, Malek Ashtar University of Technology, Tehran, Iran

Abstract

Silicon carbide is one of the most widely used ceramics due to its high compressive strength, low cost and easy access. However, high brittleness is one of the most important problems of these ceramics, which can be decreased by adding additives. In this article, the effect of adding graphene quantum dots nanoparticles has been determined. This article steps include; design of experiment, determining the best state of pressure, humidity and grinding time, and finally manufacturing samples with different percentages of graphene quantum dots up to 1% and determining the mechanical properties of the samples. The results show that in humidity of 7%, grinding time of 1 hour and pressure of 120 bar, raw compressive strength as well as raw flexural strength has its maximum value. Also adding graphene quantum dots to silicon carbide improves the mechanical properties of sintered samples to some critical limit due to the locking of grain boundaries and through mechanisms such as crack bridging and after that, it leads to a decrease in the properties. Besides, the best properties (hardness 27.90 GPa, Young's modulus 450.64 GPa and flexural strength 421 MPa) are obtained when 0.6% of GQDs is added.

Keywords:

Silicon carbide, Graphene quantum dots, Hardness, Flexural strength

* hosseinkia2006@gmail.com - tel: 00989127066272 – fax: 22935341

1- Introduction

SiC[2] has been paid attention by researchers in recent years due to its low density, high hardness, high melting temperature, high Young's modulus, low coefficient of thermal expansion, excellent thermal stability, high corrosion resistance in harsh environments, adequate thermal conductivity, outstanding creep resistance, excellent wear and oxidation resistance, and high-temperature strength [1-10]. SiC ceramics are used in many industries including wear-resistant components, refractories, semiconductor components, electronic equipment, high-temperature applications such as engines and heat exchangers, and the military and nuclear industries due to their desirable and acceptable properties [11-17].

Despite the good properties that SiC has, high brittleness and high sintering temperature are disadvantages that make its use difficult. One of the ways to overcome these problems is adding additives to SiC. One of these additives is different combinations of graphene. Graphene is a two-dimensional structure of a single layer of carbon honeycomb network. Graphene has become a unique material due to its extraordinary properties in electrical and thermal conductivity, high density and mobility of charge carriers, optical conductivity and mechanical properties [18]. Graphene is in various forms such as GPLs[3], GNPs[4], MGN[5], GNS[6], GO[7] and rGO[8] are used as an additive [19-29]. The effect of adding graphene is usually evaluated more on the electrical properties and little research has been done on the effect of graphene on the mechanical properties. However, studies show that in most ceramics, adding graphene improves mechanical properties and fracture toughness. For example, by adding a certain amount of graphene to SiC, its fracture resistance, hardness and strength can be increased, in this case, GO has been used as an additive [30]. Also, by adding GPLs to Al2O3-SiC ceramics, its mechanical properties, including bending strength, can be improved [31]. Graphene in the form of whiskers can also increase the fracture toughness of SiC. Thus, by increasing the size of graphene layers and reducing the number of layers, it is possible to achieve greater toughness [32]. In fact, graphene increases the toughness by activating the sintering field in spark plasma [33]. During the plasma arc sintering process, graphene sheets are placed in preferred

2 Silicon carbide
3 Graphene layers
4 Graphene nanoplatelets
5 Multilayer graphene nanosheets
6 Graphene nanosheets
7 Graphene oxide
8 Reduced graphene oxide

directions and will cause anisotropy in thermal conductivity [34]. Other researches have been done on improving the properties of SiC by adding graphene. Among other things, reduced graphene oxide increases the fracture toughness compared to graphene sheets [35]. The results of the experiments show that by using rGO instead of GPLs in SiC, the fracture toughness increases up to 97% [36]. Researches also show that in low weight percentages, increasing the amount of graphene increases the fracture toughness, but if the weight percentage of graphene is high (more than a critical limit), it will lead to a decrease in fracture toughness [37-38]. SiC/graphene composites can be created with one or more graphene layers, and this number of layers can affect the mechanical properties. The presence of a single layer of graphene can increase the strength and fracture strain compared to the multi-layer state. Also, with the increase in the volume fraction of graphene, the elastic modulus increases [39]. The presence of graphene nanofillers (in the form of graphene sheets or reduced graphene oxide) in the SiC field can also increase the fracture strength. Thus, by adding 20% by weight of graphene sheets (GPLs) or 5% of reduced graphene oxide (rGO), the stress distribution in the crack tip can be changed, which leads to the conicity of the crack tip and the development and it makes the crack growth in the composite problematic [40]. Another form of graphene is GQDs[9] which are very small particles of graphene that usually have dimensions below 20 nm in diameter [41]. GQDs are nanoparticles with high potential in medical and industrial applications because of their remarkable and unique properties [42].

Graphene is a single-layer material of carbon atoms and has attracted the attention of researchers due to its cross-sectional area and high load transfer capability, high flexibility and mechanical and thermal stability. On the other hand, quantum dots of semi-conducting materials are zero-dimensional and their physical properties change with particle size. These materials have suitable applications in various fields. GQDs, single or multi-layered graphene with small size is another type of quantum dots with unique properties that bring the properties of graphene and quantum dots [43-48].

As it is known, there has been no published researches on the effect of adding GQDs on the mechanical properties of SiC-based ceramics. Therefore, in this paper, firstly, the determination of the best condition of the variables like humidity, pressure, and milling time, to manufacture SiC samples with the highest compressive strength and density before sintering is discussed. Then, according to the best value of the mentioned variables, the pressureless manufacturing of SiC samples will

[9] Graphene quantum dots

be done by adding specific amounts of GQDs and finally the mechanical properties of samples with different percentages of GQDs will be discussed in order to determine its appropriate amount as an additive.

2- Experimental

2-1- Design of experiment

The most important goal of design of experiment is to achieve the best properties, by variation of the effective factors. Here are some factors to change the mechanical properties: humidity, grinding time in the mill and pressure. Each of these factors has different levels according to Table 1.

Table 1: Effective factors and their levels.

factors	Milling time (hr)	Pressure(bar)	Humidity (%)
	1	30	4
Level of	2	60	7
factors	3	90	10
		120	

The level of each factor are considered within its common experimentally range. Therefore, in each case, it is necessary to make three samples and evaluate their properties. The evaluated properties include; density, flextural strength and compressive strength are in the raw state before sintering.

Finally, after adding different amounts of GQDs, the samples (which are manufactured by the best condition of effective factors) are sintered at about 2200 °C for two hours.

2-2- Preparing samples

The SiC mesh used in this article is 2 to 3 microns. First, SiC weighted in two packages of 120 gr according to Fig 1 and put each of these two packages into special cups along with alcohol according to Fig 1 and put 6 tungsten carbide balls weighing 20 grams in each cup. It can help to grind. Then two cups are placed in the mixer and they are mixed for 1 hour at a speed of 190 rpm.

Fig1 Placing the tungsten ball inside the cup.

After finishing this step, each of 120 gr of silicon carbide is spread on aluminum foil according to Fig 2 and placed inside the oven to remove the alcohol.

Fig 2 Grinding lumped silicon carbide on aluminum foil.

During the heating process, every 20 minutes, the lumps created in the oven are crushed to finally obtain the ground powder. Finally, the remaining lumps can be removed by sieving. In the same way, SiC powder is also prepared with 2 hours and 3 hours grinding time.

After that, by mixing powder with defined amounts of humidity (4, 7 and 10), tablet-shaped samples are created through a press in a special mold (pressure: 30, 60, 90 and 120 bar). Three samples are produced for each working condition (pressure, grinding time and pressure).Finally, tablets with different grinding time, humidity and pressure are obtained. Then the samples are coded (according to Fig 3), their dimensions are measured and their raw density is determined.

Fig 3 Part of the pressed samples and their coding.

It is worth mentioning that with 11% humidity, the possibility of pressing was not provided in any of the working pressures, which shows that at this percentage of humidity and more, the possibility of pressing the sample will not be provided and the sample cannot be produced. Therefore, the total number of samples is 99.

2-3- Determination of mechanical properties and raw density

After manufacturing the samples, their dimensions (diameter and thickness) and weight are measured and their raw density is calculated. Also, for each unique state of pressure, grinding time and humidity percentage, one of the samples is subjected to a three-point bending test and another one is subjected to a compression test, and the software is adjusted in such a way that the force is recorded in terms of displacement for the samples.

Fig 4 shows the diagram of force in terms of displacement for the state of milling time of 1 hour, humidity of 4% and pressure of 30 bars.

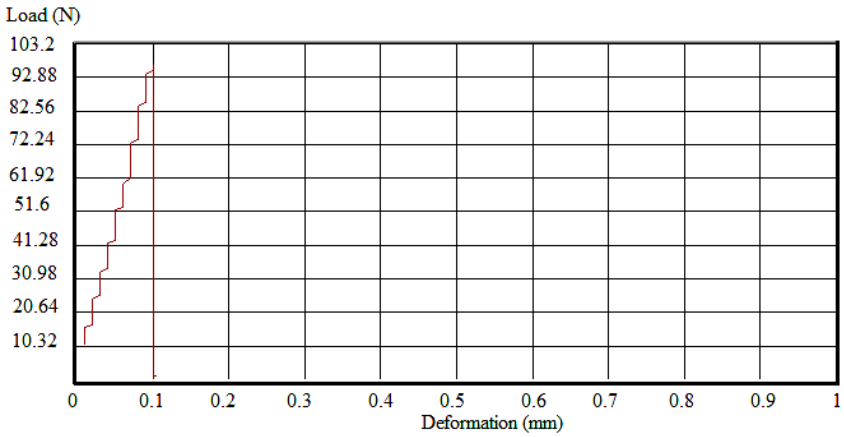

Fig 4 Force-displacement diagram for the three-point bending test of the sample with 1 hour grinding time, 4% humidity and 30 bar press pressure.

In all three-point bending tests, while entering the dimensional specifications of the samples in the software, the loading rate is set at 0.08 mm/min.

Also, in each working mode, one of the samples is also used in uniaxial pressure test. In this test, the loading rate is defined as 0.5 mm/min.

In Fig 5, the graph obtained from the pressure test, the effect of barreling (increasing the slope of the graph) is quite evident.

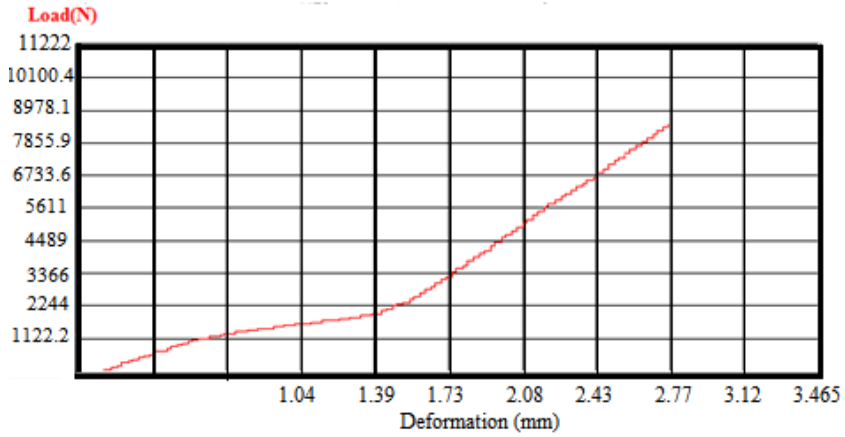

Fig 5 Force-displacement diagram for uniaxial pressure test of the sample with 1 hour milling time, 4% humidity and 30 bar press pressure.

According to the very high compressive strength of ceramics, the amount of force required to reduce the thickness of the samples to half of the initial state is considered as the end point.

2-4- Addition of GQDs

According to the fact that in the working conditions determined in the previous paragraph, the density and mechanical properties have been improved, therefore, a sample with these conditions and with the dimensions of 50x20x5 mm was manufactured and sintered for two hours in the temperature is set at 2200°C. Fig 6 shows this sample.

Fig 6 Sintered SiC sample.

Also, more samples similar to the above sample are produced with the addition of GQDs according to the percentages listed in Table 2.

Table 2: Percentage of GQDs which are used an an additive.

GQDs %	0.2
	0.4
	0.6
	0.8
	1

The synthesis of GQDs is as follows: first, citric acid was weighed and transferred into the beaker. The beaker was heated at the temperature of 200 °C for about five minutes, and the color of the solution changed from a colorless liquid to a colored one. It turned yellow. The yellow solution was neutralized with 0.21 molar sodium hydroxide solution and under intense stirring for 30 minutes, orange colored GQDs were obtained and the obtained product was dried in an oven at 110 °C for 6 hours. Then, for further purification, it was washed using 100 mg of distilled water. The color of the solution indicates the incomplete carbonization and the formation of GQDs.

Then, the resulting GQDs is added to SiC, according to the flowchart in Fig 7. Now, the sintered samples are prepared as standard samples to determine the mechanical properties.

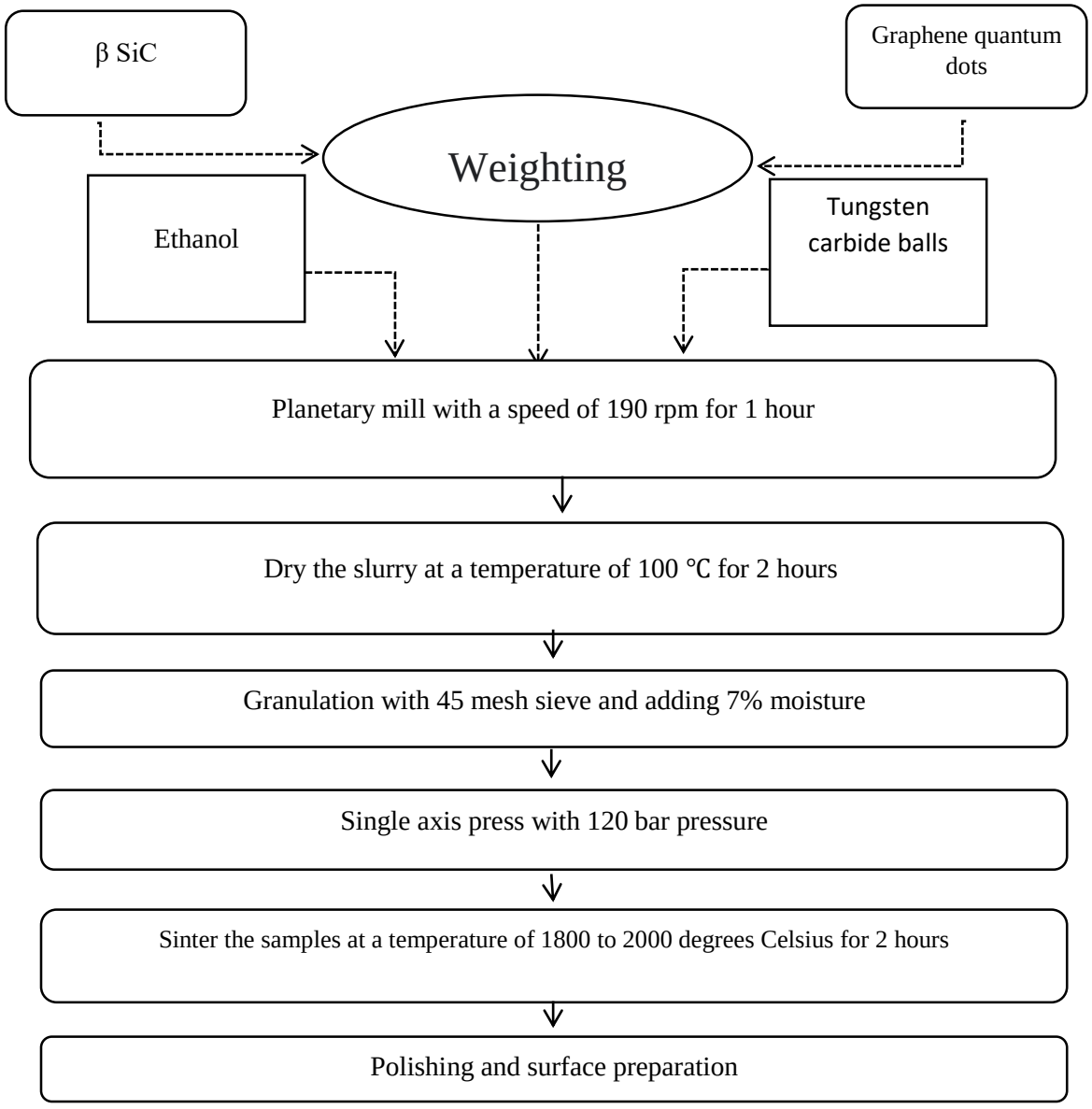

Fig 7 Fabrication method of SiC samples sintered with graphene quantum dot additive.

3- Results and discussion

Table 3 shows the density, flexural strength and compressive strength for the samples with 4% humidity, pressure of 30, 60, 90 and 120 bar, as well as grinding time of 1, 2 and 3 hours.

Table 3: Results for samples with 4% humidity.

Compressive resistance(N)	Bending fracture force (N)	Density (gr/cm^3)	Weight (gr)	Sample No.	Milling time (hr)	Press pressure (bar)
--	--	1.65	2.99	A1		
--	95	1.64	3.02	A2		*30*
8671	--	1.67	2.97	A3		
--	167	1.75	3.00	A4		
8437	--	1.75	2.99	A5		*60*
--	--	1.76	3.02	A6		
--	209	1.84	2.97	A7	١	
9404	--	1.85	3.05	A8		*90*
--	--	1.85	3.11	A9		
--	194	1.85	2.99	A10		
10396	--	1.89	3.06	A11		*120*
--	--	1.89	3.06	A12		
--	174	1.69	3.01	B1		
11165	--	1.74	2.92	B2		*30*
--	--	1.73	3.01	B3		
--	175	1.80	2.91	B4		
10412	--	1.82	2.94	B5		*60*
--	--	1.82	2.88	B6		
--	177	1.81	2.98	B7	2	
10555	--	1.84	2.91	B8		*90*
--	--	1.83	3.02	B9		
--	95	1.81	3.05	B10		
9916	--	1.80	3.03	B11		*120*
--	--	1.81	2.98	B12		
--	63	1.57	2.99	C1		
9851	--	1.64	3.02	C2		*30*
--	--	1.67	2.97	C3		
--	--	1.82	3.00	C4		
--	138	1.75	2.99	C5		*60*
10180	--	1.83	3.02	C6		
--	153	1.91	2.97	C7	3	
13436	--	1.92	3.05	C8		*90*
--	--	2.00	3.11	C9		
--	178	1.96	2.99	C10		
9363	--	2.01	3.06	C11		*120*
--	--	2.05	3.06	C12		

Table 4 shows the density, flexural strength and compressive strength for the samples with 7% humidity, pressure of 30, 60, 90 and 120 bar and grinding time of 1, 2 and 3 hours.

Table 4: Results for samples with 7% humidity.

Compressive resistance(N)	Bending fracture force (N)	Density (gr/cm^3)	Weight (gr)	Sample No.	Milling time (hr)	Press pressure (bar)
--	170	1.94	3.01	D1	1	30
11122	--	1.94	2.77	D2		
--	--	1.98	2.76	D3		
8481	--	1.96	2.43	D4		60
--	219	2.02	2.88	D5		
--	--	1.84	2.80	D6		
--	215	2.09	2.85	D7		90
10104	--	2.06	2.68	D8		
--	--	2.03	2.71	D9		
--	225	2.06	2.87	D10		120
13467	--	2.05	2.79	D11		
--	--	2.04	2.84	D12		
--	200	1.88	2.92	E1	2	30
11780	--	1.84	2.91	E2		
--	--	1.89	2.88	E3		
--	179	2.01	2.81	E4		60
10569	--	2.02	2.82	E5		
--	--	2.09	2.92	E6		
--	210	2.06	2.74	E7		90
10029	--	2.10	2.73	E8		
--	--	2.06	2.68	E9		
--	114	2.01	2.29	E10		120
8731	--	2.09	2.12	E11		
--	--	2.04	2.14	E12		
--	102	1.91	2.91	F1	3	30
8268	--	1.87	2.84	F2		
--	--	1.93	3.00	F3		
--	119	1.99	2.90	F4		60
11083	--	1.98	2.83	F5		
--	--	1.93	2.76	F6		
--	135	2.02	2.95	F7		90
12207	--	2.01	2.80	F8		
--	--	2.04	2.91	F9		
--	143	2.11	2.94	F10		120
11095	--	2.11	2.94	F11		
--	--	2.05	2.92	F12		

Table 5 shows the density, flexural strength and compressive strength for the samples with 10% humidity, pressure of 30, 60, 90 and 120 bar, as well as grinding time of 1, 2 and 3 hours.

Table 5: Results for samples with 10% humidity.

Compressive resistance(N)	Bending fracture force (N)	Density (gr/cm^3)	Weight (gr)	Sample No.	Milling time (hr)	Press pressure (bar)
--	104	1.97	2.62	G1		
9738	--	1.93	2.57	G2		*30*
--	--	1.91	2.67	G3		
--	90	2.01	2.49	G4		
--	--	1.91	2.48	G5	١	*60*
10015	--	2.05	2.28	G6		
--	129	2.08	1.45	G7		
--	--	2.07	1.31	G8		*90*
13080	--	1.87	1.78	G9		
--	67	1.97	2.69	H1		
9150	--	1.89	2.64	H2		*30*
--	--	2.01	2.74	H3		
--	105	2.05	2.47	H4		
10765	--	1.92	2.25	H5	2	*60*
--	--	2.06	2.42	H6		
--	64	2.00	2.09	H7		
9970	--	1.95	2.10	H8		*90*
--	--	2.09	1.99	H9		
--	40	1.89	2.87	I1		
10100	--	1.94	2.83	I2		*30*
--	--	1.86	2.77	I3		
--	81	1.97	2.44	I4		
8320	--	1.99	2.52	I5	3	*60*
--	--	1.99	2.52	I6		
--	91	2.03	2.38	I7		
10600	--	2.05	2.41	I8		*90*
--	--	2.08	2.44	I9		

As shown in the table 5, at 120 bar pressure and 10% humidity, the samples could not be produced. Now, by examining the effect of the three variables of grinding time, humidity percentage and pressure on the response variable, it is possible to determine the state that creates the best properties before sintering.

Fig 8 shows the simultaneous effect of the mentioned variables on the force required for the bending failure of the samples.

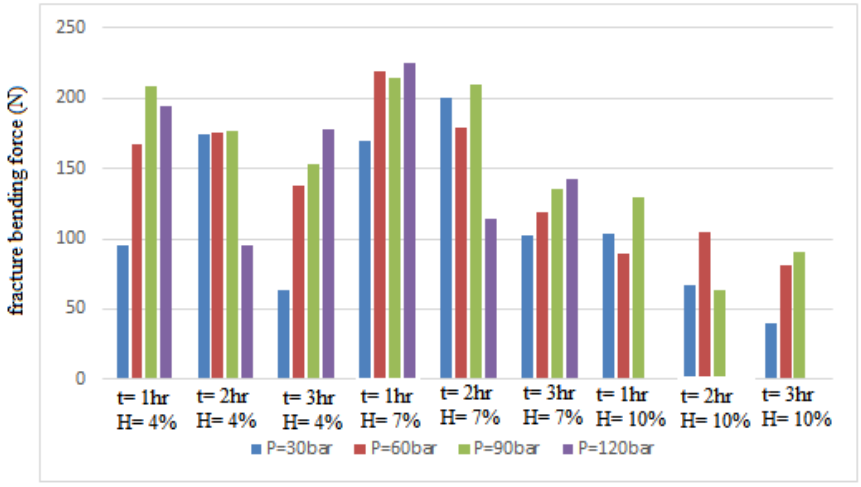

Fig 8 The effect of grinding time, humidity percentage and press pressure on the flexural strength of the silicon carbide sample.

According to fig 8, the flexural strength is higher than other conditions at 1 hour milling time, 7% humidity and 120 bar pressure. In this case, even at the pressure of 60 bar and 90 bar, the bending resistance has its maximum value, and therefore at 7% humidity and 1 hour grinding time, the best pressure should be chosen from 60 to 120 bar. Also, increasing humidity to more than 7% causes a sharp drop in flexural strength.

Fig 9 shows the simultaneous effect of the mentioned variables on the compressive force required to change the thickness of the samples to half of the initial state.

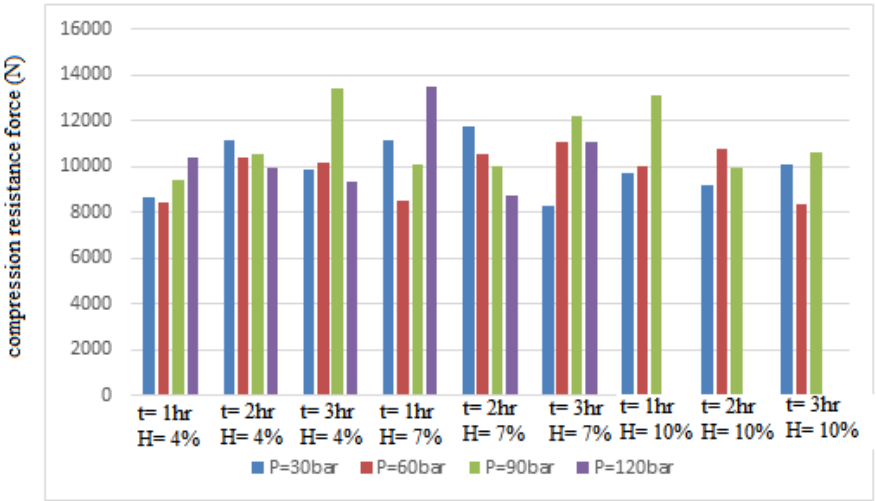

Fig 9 The effect of grinding time, humidity percentage and press pressure on the compressive strength of the silicon carbide sample.

In this case, even though in different states and conditions, the amount of changes compared to the flexural strength is less, but still, similar to the flexural strength, the compressive strength has its maximum value at 7% humidity, 1 hour grinding time, and 120 bar pressure. Fig 10 also shows the effect of mentioned variables on raw density.

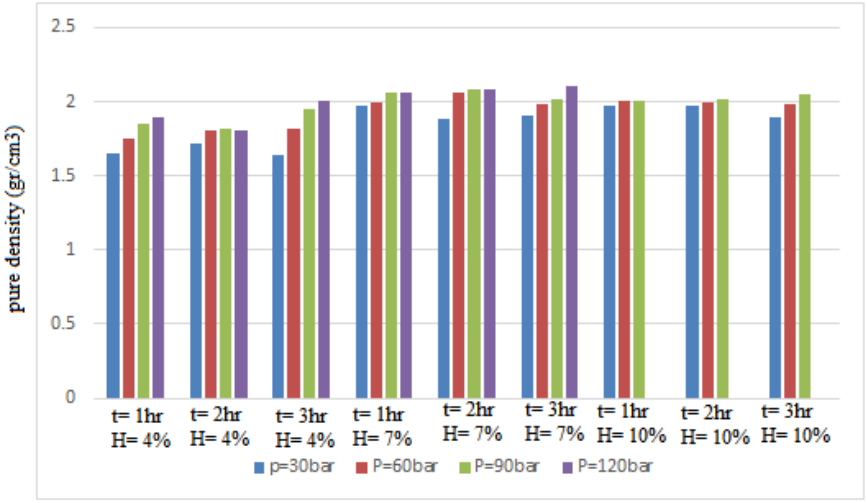

Fig 10 The effect of grinding time, moisture percentage and press pressure on the raw density of silicon carbide sample.

Fig 10 shows that the maximum raw density is obtained at 7% humidity and pressure above 60 bar.

In order to more accurately evaluation of the effect of humidity, grinding time and press pressure on the response variables including raw density, compressive strength and bending strength, factorial design is used.

Using Minitab software and based on the principle of randomization of sample production with the method of factorial test design, the effect of the main factors on the flexural strength variable has been shown in Fig 11.

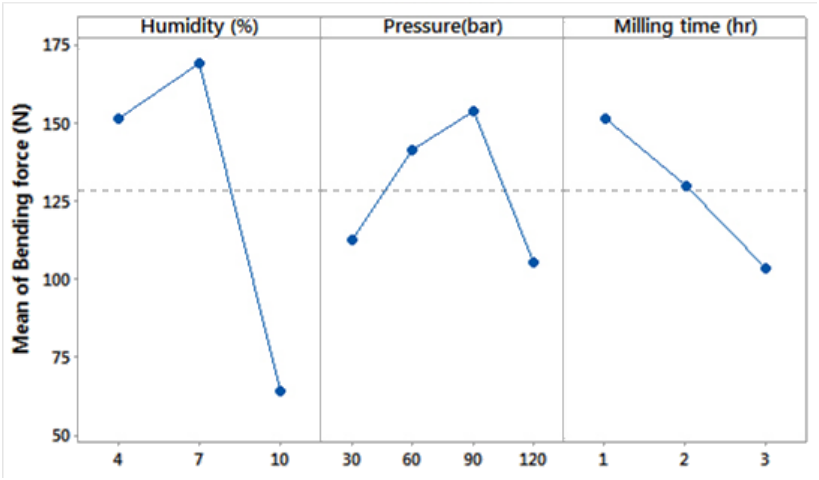

Fig 11 The effect of the main factors on the flexural strength variable.

As shown in Fig 11, pressure and humidity both increase the flexural strength to some critical limit and then have a decreasing effect. But increasing the grinding time the flexural strength decreases.

Considering the compressive strength as the response variable in the factorial test plan, the effect of the main factors on it has been shown in Fig 12.

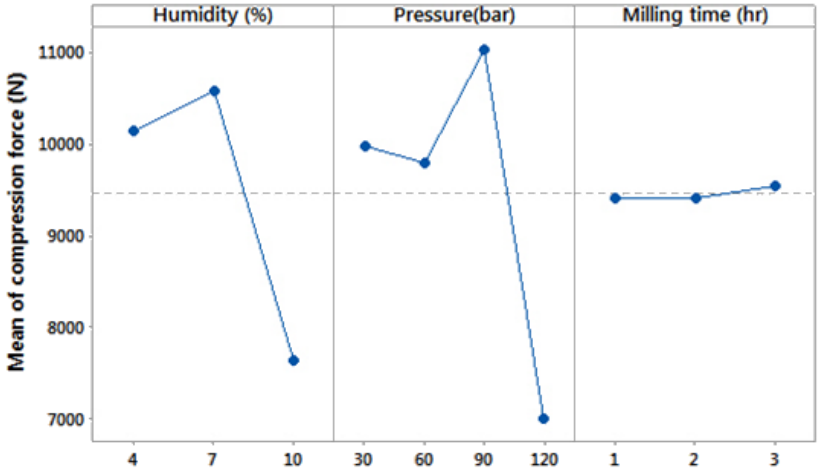

Fig 12 The effect of the main factors on the compressive strength variable.

As shown in Fig 12, pressure and humidity both increase the compressive strength to some extent and then have a decreasing effect. But increasing the grinding time does not have a significant effect on the compressive strength.

Fig 13 shows the effect of the main factors on the raw density variable.

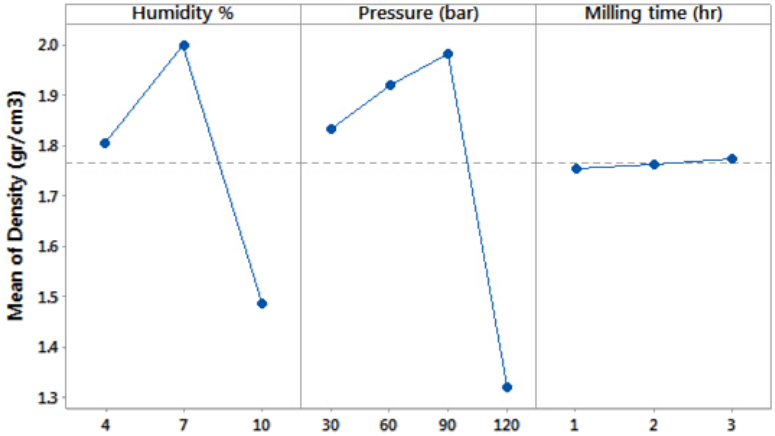

Fig 13 The effect of the main factors on the raw density variable.

As shown in Fig 13, pressure and humidity both increase the compressive strength to some extent and then have a decreasing effect. But increasing the grinding time does not have a significant effect on the compressive strength.

In fact, it has been indicated from Figs 11, 12 and 13 that with the increase of the pressure, the mechanical properties become better due to the denser powder. But from a certain point onwards, the creation of microcracks caused by the excessive increase in pressure can cause a drop in mechanical properties. An increase in humidity to a certain extent improves the mechanical properties and pressability, but after a certain point, along with the drying of the samples, the humidity appears in the interior of the sample in the form of prosity and voids and so causes a decrease in properties. Regarding the milling time, it also appears that its effect is less than the humidity and pressure. However, an excessive increase in milling time can also lead to a loss of properties by disrupting the granulation and morphology of the particles (according to Fig 11).

Therefore, the obtained results shown that the sample with the best density and mechanical properties is obtained with the working conditions of 120 bar pressure, 1 hour grinding time and 7% humidity. Therefore, a sample with these conditions and dimensions of 50x20x5 mm has been manufactured and sintered at about 2200°C for 2 hours.

Then, these sintered samples with different percentages of GQDs has been prepared as standard samples of hardness, flexural strength, etc., and the corresponding properties have been determined. The properties of sintered samples are as described in Table 6. It is worth mentioning that density has been determined by Archimedes method and hardness obtained based on ASTM C1327 standard. Also, Young's modulus has been calculated and determined based on the ASTM C769 standard and based on the speed of sound obtained by the TC600 thickness gauge.

Table 6 Final properties of SiC sintered with working conditions of 7% humidity, grinding time of one hour and pressure of 120 bar, sintered at a temperature of 2200 °C with different percentage of GQDs.

GQD%	0	0.2	0.4	0.6	0.8	1
Density (gr/cm3)	3.04	3.06	3.07	3.09	3.05	3.04
Young's modulus (GPa)	423.86	435.14	442.81	450.64	434.76	428.61
Hardness (GPa)	25.68	26.41	26.85	27.90	26.39	25.93
Sound speed (m/s)	11808	11925	12010	12074	11939	11874
Flexural Strength (MPa)	356	381	395	421	390	383

As shown in above table, in the sample without GQDs, a density of about 97% of the theoretical value was obtained and other mechanical properties are also very suitable and in accordance with the nominal values. Also, increasing the percentage of GQDs leads to the improvement of properties, and after some critical amount, it leads to a decrease in properties. Besides, the best properties were obtained when about 0.6% of GQDs has been added.

Fig 14 shows the effect of adding deferent percent of GQDs to SiC properties.

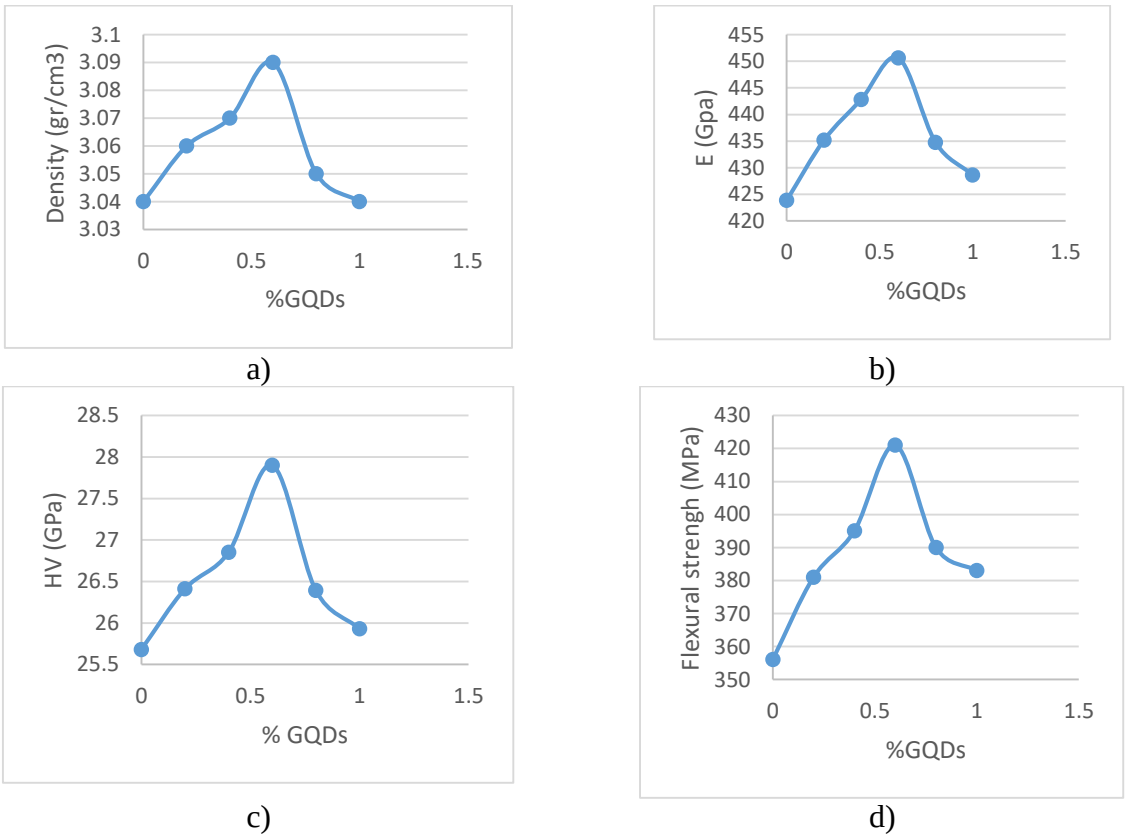

Fig 14 effect of adding deferent percent of GQDs to SiC a) density b) Young′s modules c) Vickers hardness and d) flexural strength.

Table 7, shows the average and also standard deviation for each parameters

.

Table 7: average and standard deviation of density, hardness, Young's modules and Flexural strength.

Parameters	Average	Standard deviation
Density (gr/cm3)	3.058333	0.019408
Young's modulus (GPa)	435.97	9.643331
Hardness (GPa)	26.52667	0.786859
Flexural Strength (MPa)	387.6667	21.16286

In Fig 15, the X-ray diffraction (XRD) pattern of samples containing 0% and 1% by weight of GQDs additive is presented. As can be seen, in the sample without graphene, the structure only includes the dominant phase of SiC. While in the sample containing 1% by weight of GQDs, in addition to the dominant phase of SiC, the peak corresponding to graphene is also observed at the angle of 2θ=27. Also, this fig shows that no new phase is formed by adding graphene to the SiC background. It is not found that this is due to the good compatibility of graphene and SiC at temperatures higher than 2130 °C. In other words, at high temperatures, graphene and SiC have no reaction with each other.

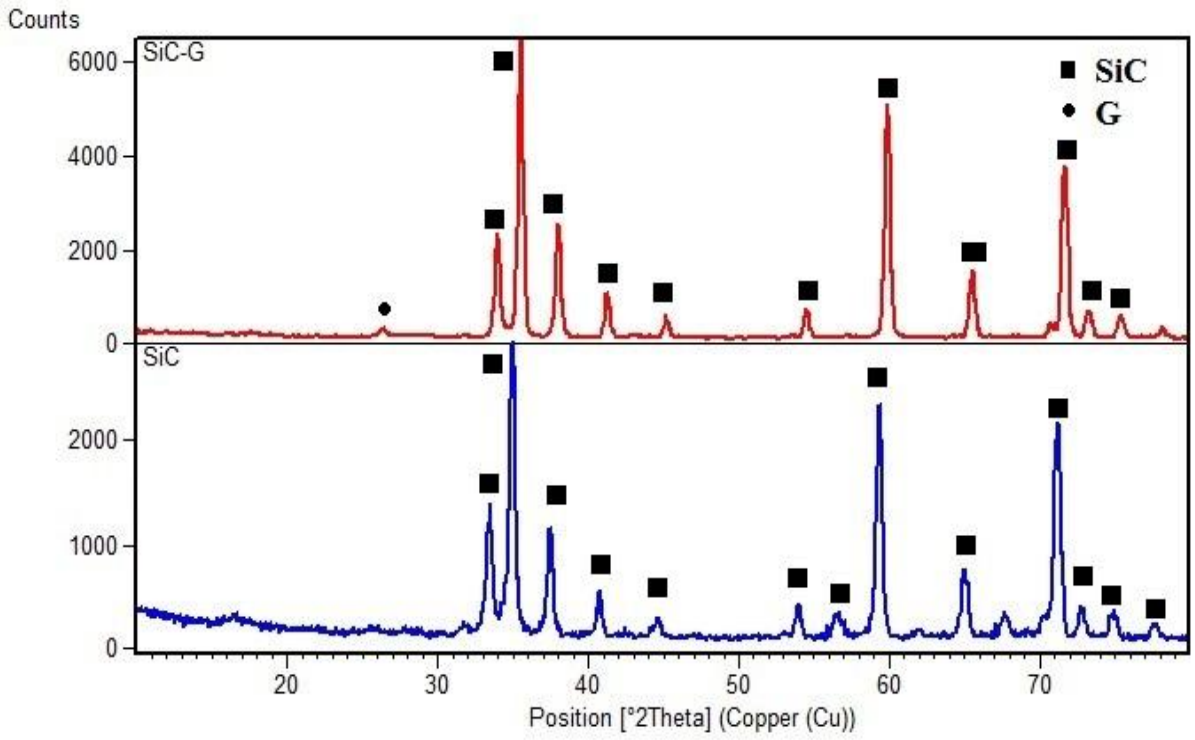

Fig 15 XRD patterns of sintered samples a) 0% b) 1% GQDs.

Fig 16 shows the SEM image of the sample containing 0.2 wt% GQDs. Fig 17 also shows the EDS analysis of SiC samples containing 0.2% GQDs.

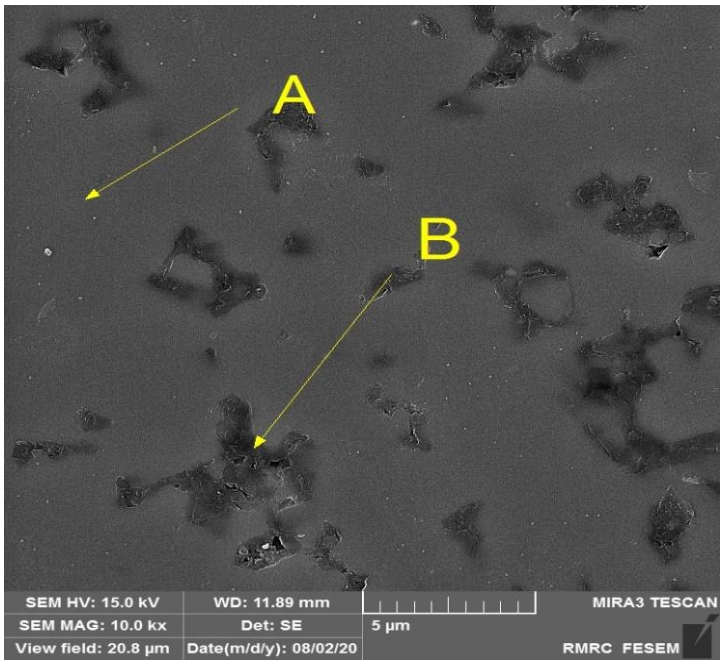

Fig 16 SEM image of the distribution of 0.2% GQDs on the SiC substrate

According to Fig 17, the matrix phase (A) shows the presence of a large amount of Si, so it can be said that part A is related to the SiC phase. Also, the darker parts (B) that have been created as a mass have a higher amount of carbon. Therefore, according to the presence of carbon in this part, it can be said that part B is related to the graphene phase.

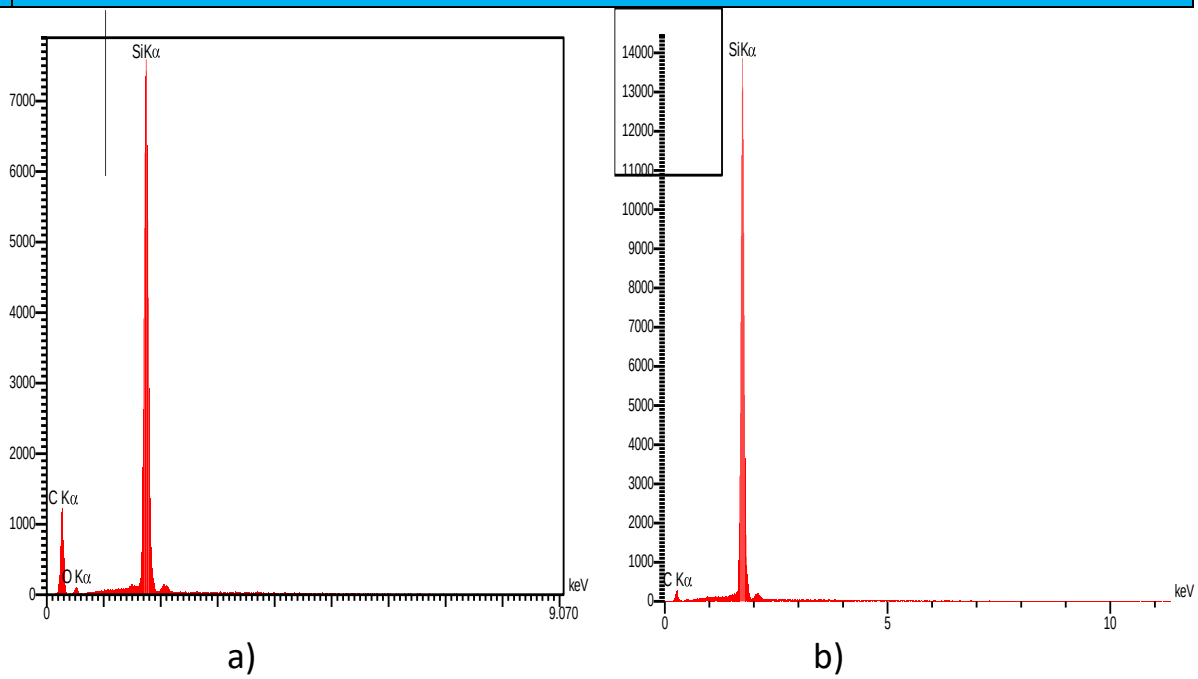

Fig 17 EDS diagram of a) matrix phase b) reinforcing phase

The dot map analysis of the composition containing 1% by weight of GQDs is shown in Fig 18. As can be seen, the graphene phase is relatively homogeneously distributed in the SiC phase.

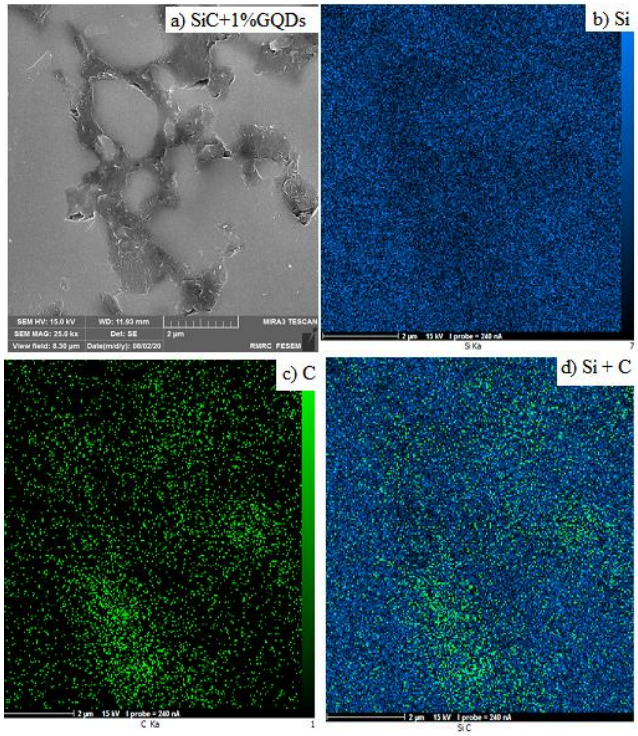

Fig 18 Carbon distribution in SiC containing 1% GQDs a) SEM image b) Si point map analysis c) C dot map analysis d) Si and C dot map analysis.

In Fig 19, Line analysis of the sample containing 1 weight percent of graphene additive is shown. As it can be seen, in this picture, he checked 20 points of the graph. At the beginning and end points of the diagram, Si and C elements are present in the same amount, which indicates SiC in this part. And in the middle points, the carbon element has reached its highest level and Si has decreased sharply, which indicates the presence of GQDs in this part.

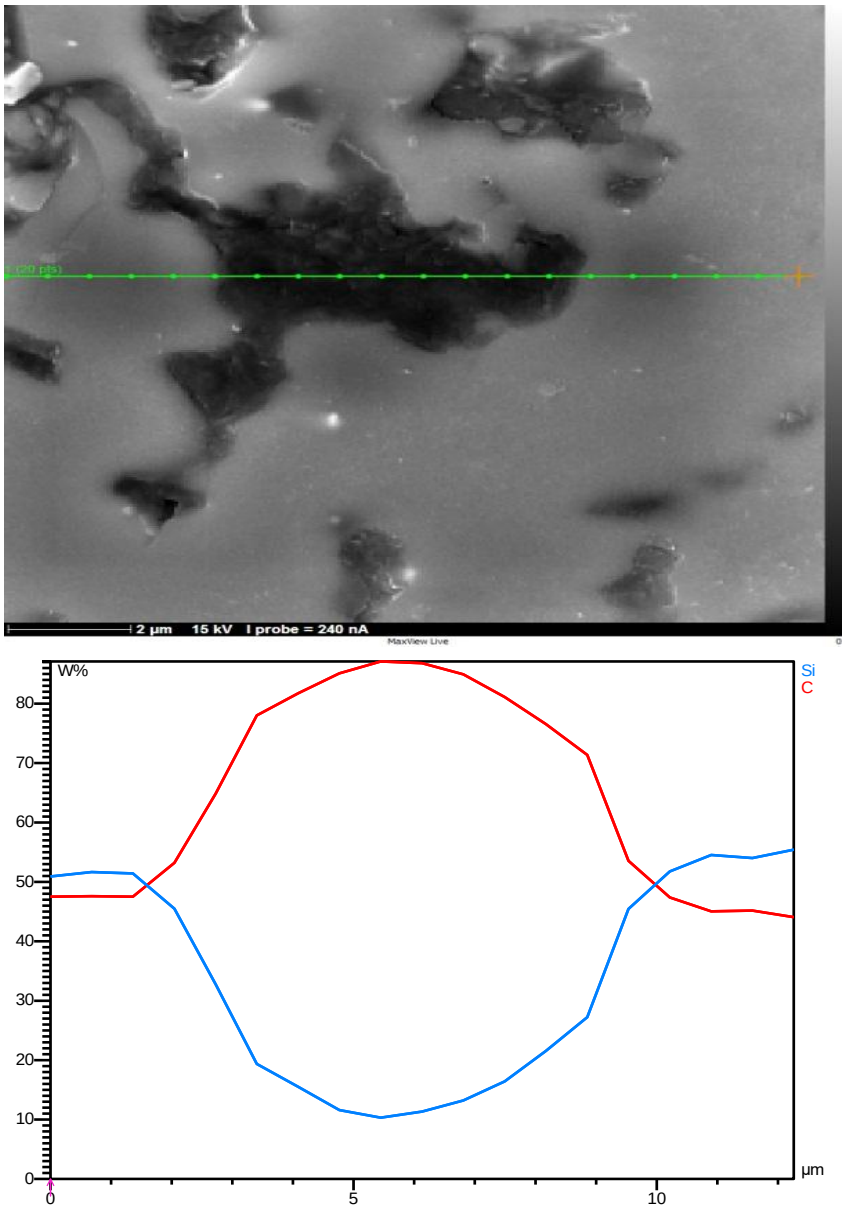

Fig 19 Line analysis of the sample containing 1% by weight of GQDs additive.

Fig 20 shows how the graphene phase is distributed in the SiC phase.

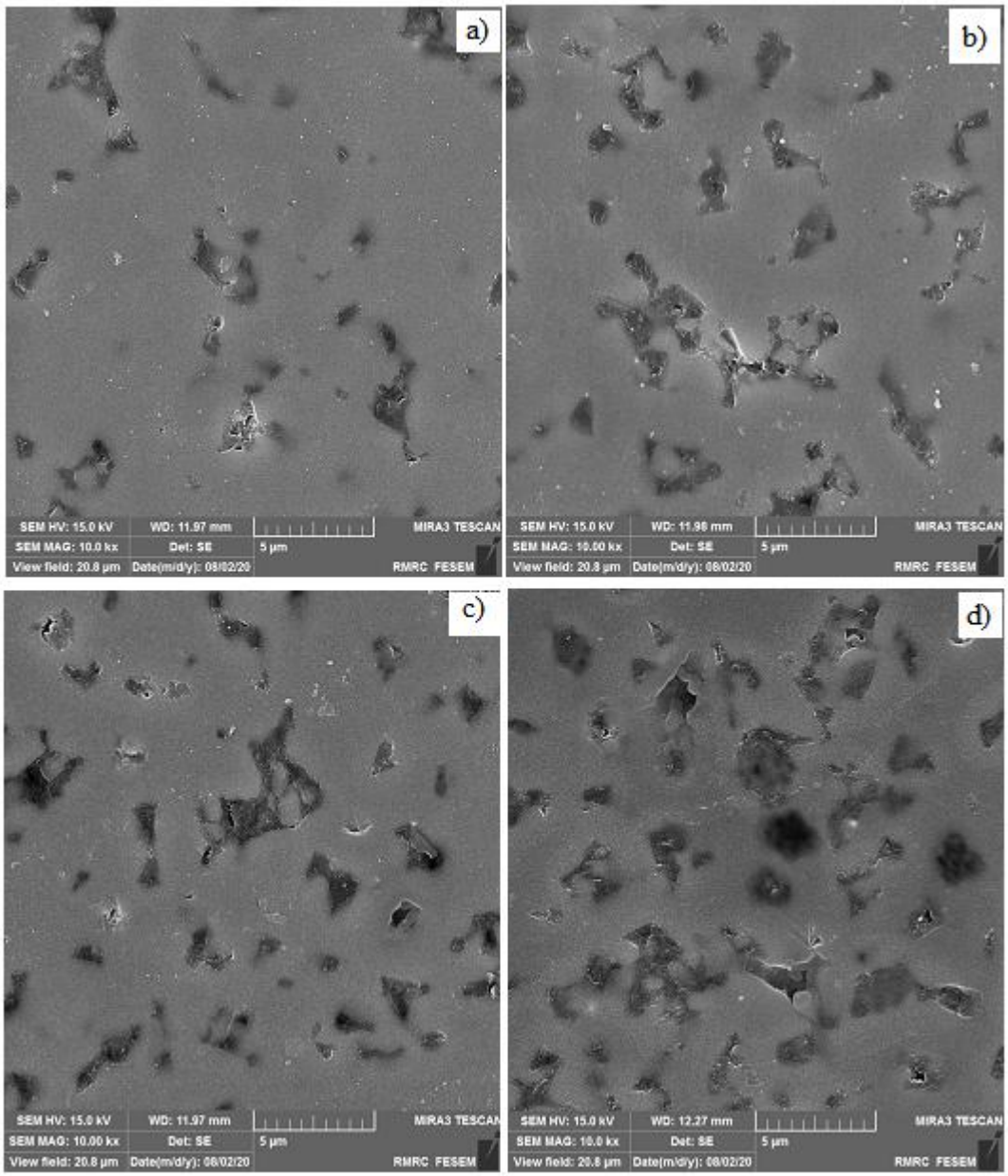

Fig 20 Graphene phase distribution in sintered samples containing a) 0.2% b) 4% c) 0.6% d) 0.8% GQDs.

According to Fig 20, by adding GQDs up to about 0.6% by weight, the reinforcing phase is uniformly distributed in the field and the amount of graphene is low, but with an increase of up to 1% by weight, the reinforcing phase (GQDs) is agglomerated in the grain boundaries.

Fig 21 shows the effect of different amounts of GQDs on the size of SiC grains.6

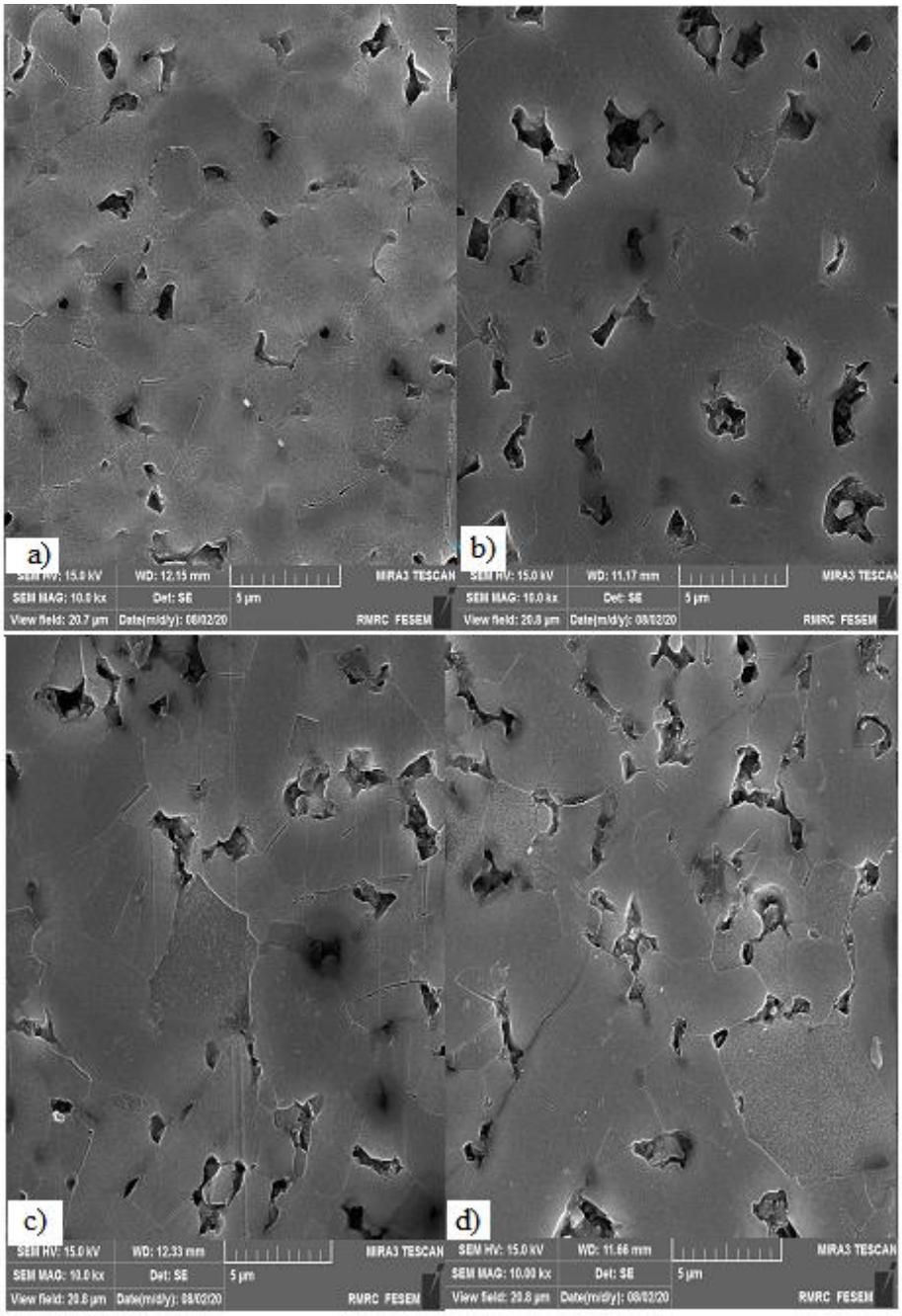

Fig 21 SEM images of the microstructure of sintered samples containing a) 0.2% b) 0.4% c) 06% d) 0.8% GQDs.

As can be seen, with the addition of GQDs up to about 0.6% by weight, a slight increase in the size of SiC grains has occurred, while with the addition of GQDs up to 1% by weight, growth of SiC grains has increased and also the porosity has increased. Among the reasons for grain growth in this research, high sintering temperature and pressureless method, which can achieve higher mechanical properties by using other sintering methods such as SPS and hot press.

With the increase in the amount of graphene in the SiC field, the graphene particles prevent the mass transfer and this has led to a decrease in the density and an increase in the porosity of the samples from a critical point onwards, thus causing the growth of SiC grains. Therefore, it can be concluded that the addition of GQDs up to about 0.6% due to the locking of the grain boundaries and preventing its excessive growth, as well as the activation of mechanisms such as crack bridging and crack branching, leads to the improvement of strength, hardness and Young's modulus. But with the increase of GQDs more than 0.6%, firstly, due to the creation of porosity, the density decreases and the speed of sound decreases. According to the relationship between sound speed and Young's modulus, a decrease in the amount of elastic modulus of the samples is also observed. Secondly, due to the increase in the amount of graphene, the phenomenon of agglomeration occurs and causes the growth of grains, which results in a decrease in mechanical properties.

4- Conclusion

The following result has been obtain from experimental tests:

- At humidity levels above 10%, the sample lacks manufacturability or cracked samples are created.
- At 7% humidity and pressure above 60 bar, the maximum raw density was obtained.
- In humidity of 7%, grinding time of 1 hour and press pressure of 120 bar, compressive strength as well as bending strength has been reached its maximum value.
- By increasing the pressure, the mechanical properties become better due to the denser powder. But from a certain point onwards, the creation of microcracks caused by the excessive increase in pressure has been caused a drop in mechanical properties.
- Increasing the humidity to a certain extent has been improved the mechanical properties and pressability, but after a certain point, along with the drying of the samples, the humidity has been appeared in the interior of the sample in the form of mucus and holes and caused a decrease in properties.

- Regarding the milling time, it also has been determined that its effect was less than the humidity and press pressure. However, an excessive increase in milling time could also lead to a loss of properties by disrupting the granulation and morphology of the particles
- According to the best manufacturing conditions mentioned before, it is possible to manufacture samples with different dimensions, and then the samples are transferred to the hot sintering stage for final processing. After sintering at 2200 degrees Celsius, such a sample will have suitable mechanical properties (hardness 25.68 GPa, modulus 423.86 GPa, and flexural strength 356 GPa) and a density of about 97% of the nominal value. .
- Increasing the percentage of GQDs has been resulted to the improvement of the properties, and after some critical value (about 0.6 wt%) , a decrease in the properties has been observed. Besides, the best properties (hardness 27.90 GPa, modulus 450.64 GPa and flexural strength 421 GPa) were obtained when 0.6% of GQDs was added.

Declaration of interests

The authors declare that they have no known competing financial interests or personal relationships that could have appeared to influence the work reported in this paper.

References

[1] W. Chi, D. Jiang, Z. Huang, S. Tan, Sintering behavior of porous SiC ceramics, Ceramics International, 30(6) (2004) 869-874.

[2] B. K. Jang, Y. Sakka, Thermophysical properties of porous SiC ceramics fabricated by pressureless sintering, Science and Technology of Advanced Materials, 8(7-8) (2007) 655.

[3] S. Kultayeva, J.-H. Ha, R. Malik, Y.-W. Kim, K.J. Kim, Effects of porosity on electrical and thermal conductivities of porous SiC ceramics, Journal of the European Ceramic Society, 40(4) (2020) 996-1004.

[4] B.M. Kumar, Y.-W. Kim, D.-S. Lim, W.-S. Seo, Influence of small amount of sintering additives on unlubricated sliding wear properties of SiC ceramics, Ceramics International, 37(8) (2011) 3599-3608.

[5] C. Li, S. Li, D. An, Z. Xie, Microstructure and mechanical properties of spark plasma sintered SiC ceramics aided by B4C, Ceramics International, 46(8) (2020) 10142-10146.

[6] H. Liang, X. Yao, J. Zhang, X. Liu, Z. Huang, Low temperature pressureless sintering of α-SiC with Al2O3 and CeO2 as additives, Journal of the European Ceramic Society, 34(3) (2014) 831-835.

[7] K. Negita, Effective sintering aids for silicon carbide ceramics: reactivities of silicon carbide with various additives, Journal of the American Ceramic Society, 69(12) (1986) C-308-C-310.

[8] N. Song, H.-b. Zhang, H. Liu, J.-z. Fang, Effects of SiC whiskers on the mechanical properties and microstructure of SiC ceramics by reactive sintering, Ceramics International, 43(9) (2017) 6786-6790.

[9] T.T. Xu, S. Cheng, L.Z. Jin, K. Zhang, T. Zeng, High-temperature flexural strength of SiC ceramics prepared by additive manufacturing, International Journal of Applied Ceramic Technology, 17(2) (2020) 438-448.

[10] T. Zhang, Z. Zhang, J. Zhang, D. Jiang, Q. Lin, Preparation of SiC ceramics by aqueous gelcasting and pressureless sintering, Materials Science and Engineering: A, 443(1-2) (2007) 257-261.

[11] T. Koyanagi, Y. Katoh, T. Nozawa, L.L. Snead, S. Kondo, C.H. Henager Jr, M. Ferraris, T. Hinoki, Q. Huang, Recent progress in the development of SiC composites for nuclear fusion applications, Journal of Nuclear Materials, 511 (2018) 544-555.

[12] J. Das, P. Patel, J.J. Reddy, V.B. Prasad, Microstructure and mechanical properties of a SiC containing advanced structural ceramics, International Journal of Refractory Metals and Hard Materials, 84 (2019) 105030.

[13] M. Lopez-Robledo, A. Gómez-Martín, J. Ramírez-Rico, J. Martínez-Fernández, Sliding wear resistance of porous biomorphic sic ceramics, International Journal of Refractory Metals and Hard Materials, 59 (2016) 26-31.

[14] M. Bondioli, C. Santos, K. Strecker, E. Lima, M.P. da Silva, R. Magnago, Oxidation behavior of LPS-SiC ceramics sintered with AlN/Y2O3 as additive, International Journal of Refractory Metals and Hard Materials, 42 (2014) 246-254.

[15] A. Kovalčíková, P. Kurek, J. Balko, J. Dusza, P. Šajgalík, M. Mihaliková, Effect of the counterpart material on wear characteristics of silicon carbide ceramics, International Journal of Refractory Metals and Hard Materials, 44 (2014) 12-18.

[16] J. Zhang, D. Jiang, Q. Lin, Z. Chen, Z. Huang, Properties of silicon carbide ceramics from gelcasting and pressureless sintering, Materials & Design (1980-2015), 65 (2015) 12-16.

[17] Y.H. Kim, Y.W. Kim, K.J. Kim, Electrically conductive SiC ceramics processed by pressureless sintering, International Journal of Applied Ceramic Technology, 16(2) (2019) 843-849.

[18] Novoselov, K.S., Geim, A.K., Morozov, S.V., Jiang, D., Katsnelson, M.I., Grigorieva, I.V., Dubonos, S.V. and Firsov, A.A., 2005. Two-dimensional gas of massless Dirac fermions in graphene. nature, 438(7065),197-200.

[19] Wang, K., Wang, Y., Fan, Z., Yan, J., & Wei, T.. Preparation of graphene nanosheet/alumina composites by spark plasma sintering. Materials Research Bulletin, 46 (2011), 315-318.

[20] Walker, L. S., Marotto, V. R., Rafiee, M. A., Koratkar, N., & Corral, E. L. (2011). Toughening in graphene ceramic composites. ACS nano, 5(4), 3182-3190.

[21] Fan, Yuchi, Lianjun Wang, Jianlin Li, Jiaqi Li, Shikuan Sun, Feng Chen, Lidong Chen, and Wan Jiang. "Preparation and electrical properties of graphene nanosheet/Al2O3 composites." Carbon 48, no. 6 (2010): 1743-1749.

[22] Belmonte, Manuel, Andrés Nistal, Pierre Boutbien, Benito Román-Manso, María I. Osendi, and Pilar Miranzo. "Toughened and strengthened silicon carbide ceramics by adding graphene-based fillers." Scripta Materialia 113 (2016): 127-130.

[23] H. Porwal, P. Tatarko, R. Saggar, S. Grasso, M. Kumar Mani, I. Dlouh´y, J. Dusza,M.J. Reece, “Tribological properties of silica-graphene nano-plateletcomposites”, Ceram. Int. 40 (2014), 12067–12074.

[24] Ramirez, C., L. Garzón, P. Miranzo, M. I. Osendi, and C. Ocal. "Electrical conductivity maps in graphene nanoplatelet/silicon nitride composites using conducting scanning force microscopy." Carbon 49, no. 12 (2011): 3873-3880.

[25] Rutkowski, Paweł, Aleksandra Dubiel, Wojciech Piekarczyk, Magdalena Ziąbka, and Ján Dusza. "Anisotropy in thermal properties of boron carbide–graphene platelet composites." Journal of the European Ceramic Society 36, no. 12 (2016): 3051-3057.

[26] Kovalčíková, A., R. Sedlák, P. Rutkowski, and J. Dusza. "Mechanical properties of boron carbide+ graphene platelet composites." Ceramics International 42, no. 1 (2016): 2094-2098.

[27] Kvetková, Lenka, Annamária Duszová, Pavol Hvizdoš, Ján Dusza, Péter Kun, and Csaba Balázsi. "Fracture toughness and toughening mechanisms in graphene platelet reinforced Si3N4 composites." Scripta Materialia 66, no. 10 (2012): 793-796.

[28] Porwal, Harshit, Salvatore Grasso, and M. J. Reece. "Review of graphene–ceramic matrix composites." Advances in Applied Ceramics 112, no. 8 (2013): 443-454.

[29] Miranzo, Pilar, Cristina Ramírez, Benito Román-Manso, Luis Garzón, Humberto R. Gutiérrez, Mauricio Terrones, Carmen Ocal, M. Isabel Osendi, and Manuel Belmonte. "In situ processing of electrically conducting graphene/SiC nanocomposites." Journal of the European Ceramic Society 33, no. 10 (2013): 1665-1674.

[30] Sedlák, Richard, Alexandra KovalĽíková, Vladimír Girman, Erika Múdra, Paweł Rutkowski, Aleksandra Dubiel, and Ján Dusza. "Fracture characteristics of SiC/graphene platelet composites." Journal of the European Ceramic Society 37, no. 14 (2017): 4307-4314.

[31] Grigoriev, S., P. Peretyagin, Antón Smirnov, W. Solis, Luis A. Díaz, Adolfo Fernández, and Ramón Torrecillas. "Effect of graphene addition on the mechanical and electrical properties of Al2O3-SiCw ceramics." Journal of the European ceramic society 37, no. 6 (2017): 2473-2479.

[32] Wang, YongChao, YinBo Zhu, ZeZhou He, and HengAn Wu. "Multiscale investigations into the fracture toughness of SiC/graphene composites: Atomistic simulations and crack-bridging model." Ceramics International 46, no. 18 (2020): 29101-29110.

[33] Petrus, Mateusz, J. Wozniak, Tomasz Cygan, B. Adamczyk-Cieslak, Marek Kostecki, and Andrzej Olszyna. "Sintering behaviour of silicon carbide matrix composites reinforced with multilayer graphene." Ceramics International 43, no. 6 (2017): 5007-5013.

[34] Román-Manso, Benito, Yoan Chevillotte, M. Isabel Osendi, Manuel Belmonte, and Pilar Miranzo. "Thermal conductivity of silicon carbide composites with highly oriented graphene nanoplatelets." Journal of the European Ceramic Society 36, no. 16 (2016): 3987-3993.

[35] Belmonte, Manuel, Andrés Nistal, Pierre Boutbien, Benito Román-Manso, María I. Osendi, and Pilar Miranzo. "Toughened and strengthened silicon carbide ceramics by adding graphene-based fillers." Scripta Materialia 113 (2016): 127-130.

[36] Huang, Yihua, Dongliang Jiang, Xianfeng Zhang, Zhenkui Liao, and Zhengren Huang. "Enhancing toughness and strength of SiC ceramics with reduced graphene oxide by HP sintering." Journal of the European Ceramic Society 38, no. 13 (2018): 4329-4337.

[37] Meng, Qinghua, Bo Li, Teng Li, and Xi-Qiao Feng. "A multiscale crack-bridging model of cellulose nanopaper." Journal of the Mechanics and Physics of Solids 103 (2017): 22-39.

[38] Meng, Qinghua, and Tiejun Wang. "An improved crack-bridging model for rigid particle-polymer composites." Engineering Fracture Mechanics 211 (2019): 291-302.

[39] Belmonte, Manuel, Pilar Miranzo, and M. Isabel Osendi. "Contact damage resistant SiC/graphene nanofiller composites." Journal of the European Ceramic Society 38, no. 1 (2018): 41-45.

[40] Cheng, Yehong, Ping Hu, Shanbao Zhou, Xinghong Zhang, and Wenbo Han. "Using macroporous graphene networks to toughen ZrC–SiC ceramic." Journal of the European Ceramic Society 38, no. 11 (2018): 3752-3758.

[41] Zhang, Zhipan, Jing Zhang, Nan Chen, and Liangti Qu. "Graphene quantum dots: an emerging material for energy-related applications and beyond." Energy & Environmental Science 5, no. 10 (2012): 8869-8890.

[42] Sengupta, Shuvam, Somyajit Pal, Aritra Pal, Subhajit Maity, Kunal Sarkar, and Madhusudan Das. "A review on synthesis, toxicity profile and biomedical applications of graphene quantum dots (GQDs)." Inorganica Chimica Acta (2023): 121677.

[43] Fang, Cong, Weining Lei, Tianle Xu, Haoyu Zhong, Bin He, Linglei Kong, and Yiliang He. "Effect of reverse pulse current density on microstructure and properties of supercritical Ni-GQDs nanocomposite coatings." Electrochemistry Communications 160 (2024): 107680.

[44] Huang, Yong, Danping Wang, Yali Wei, Xin Dong, Rong Yang, Haoyun Li, Minqi Wei, Jie Yu, Lisheng Zhong, and Yunhua Xu. "Advances in synthesis of the graphene quantum dots from varied raw materials." Arabian Journal of Chemistry (2023): 105533.

[45] Huang, Yong, Danping Wang, Yali Wei, Xin Dong, Rong Yang, Haoyun Li, Minqi Wei, Jie Yu, Lisheng Zhong, and Yunhua Xu. "Advances in synthesis of the graphene quantum dots from varied raw materials." Arabian Journal of Chemistry (2023): 105533.

[46] Rao, Akshatha A., Santhosh Narendhiran, and Manoj Balachandran. "Fossil fuel derived GQD as a photosensitizer in dye-sensitized solar cells." Materials Letters 357 (2024): 135692.

[47] Gao, Feng, Yun-hao Zang, Yan Wang, Chun-qian Guan, Jiang-ying Qu, and Ming-bo Wu. "A review of the synthesis of carbon materials for energy storage from biomass and coal/heavy oil waste." New Carbon Materials 36, no. 1 (2021): 34-48.

[48] Kansara, Vrushti, Sanjay Tiwari, and Mitali Patel. "Graphene quantum dots: A review on the effect of synthesis parameters and theranostic applications." Colloids and Surfaces B: Biointerfaces 217 (2022): 112605.